Wetlands (2013) 33:617–629
DOI 10.1007/s13157-013-0418-9

ARTICLE

# Detecting Shoreline Changes in Typical Coastal Wetlands of Bohai Rim in North China

**Yuandong Wang · Xiyong Hou · Ping Shi · Liangju Yu**

Received: 5 January 2013 / Accepted: 21 March 2013 / Published online: 10 April 2013


**Abstract** Coastal wetland shoreline change represents one of the most important land-ocean interaction processes in complex and dynamic coastal environment. This paper presents the detecting of shoreline changes in four typical coastal wetlands of ecological importance along Bohai rim based on multi-temporal shorelines extracted from obtained Normalized Difference Water Index (NDWI) images using automatic binarization algorithm. Results showed that although there were statistical uncertainties dominant trends of the shoreline changes could be detected and sections that had significant area changes could be identified from satellite images. The reasons for corresponding changes occurred in these wetlands were stated in terms of natural processes and anthropogenic activities. It is our anticipation that this work would help future studies to reveal the regional/national pattern of wetland changes and support wetland protection and management in China's coast zone.

**Keywords** Ecology · Coastal wetlands · Shoreline change · Remote sensing

## Introduction

Wetlands are areas of marsh, fen, peat land or water, whether natural or artificial, permanent or temporary, with water that is static or flowing, fresh, brackish or salt, including areas of marine water the depth of which at low tide does not exceed 6 m (Ramsar 2012). Coastal wetlands are important geographical areas because of their unique floral and faunal characteristics and they constitute an important component of world coastal ecology (Kuleli et al. 2011). They also provide critical ecosystem services, fulfil important socio-economic and environmental functions, and support coastal livelihoods with valuable natural resources (fish, timber, food, oil, water et al.)(Liu et al. 2010; Rahman et al. 2011; Ramsar 2012; Delgado and Marin 2013). Shoreline of coastal wetlands is essential for wetland management activities like wetland mapping and boundary determination. Shoreline location and the changing position of this boundary though time are of elemental importance to coastal wetland scientists, and managers. In recent decades, due to the impact of various natural and human induced factors such as winds, storms, near shore currents, relative sea level rise, coastal engineering, land claim, construction of dams or reservoir, grudging, mining and water extraction, coastal wetland are suffering great pressure. As a result, shoreline of coastal wetlands could behave significant morphological changes over time.

Acquisition of shoreline information is fundamental for addressing coastal wetland problems, measuring and characterizing wetland and water resources, such as the area changes of wetlands, and the movement of its position. Remote sensing data had proved to be a unique tool for detecting coastal or deltaic wetland changes in previous researches. For example, Jiang et al. (2003) monitored shoreline changes along Bohai bay muddy wetland area in China. Genz et al. (2007) measured coast beach variations based on remote images in Hawaii. Ghanavati et al. (2008) used Landsat TM and ETM data to determine geomorphologic changes of Hendijan River Delta, south western Iran. Rebelo et al. (2009) used remote sensing (RS) and geographical information system (GIS) for wetland inventory, mapping and change analysis. Li and Michiel (2010) carried out successful studies on shoreline changes in the Pearl

Y. Wang (✉) · X. Hou · P. Shi · L. Yu
Yantai Institute of Coastal Zone Research, Chinese Academy of Sciences, No. 17, Chuihui Road, 264003, Yantai, China
e-mail: ydwang@yic.ac.cn

Y. Wang
University of Chinese Academy of Sciences, No. 19, Yuquan Road, 100049, Beijing, China

River delta wetlands and estuary. Cui and Li (2011) also monitored the dynamic shoreline change by remote sensing in the Yellow River Delta wetlands. Allard et al. (2012) investigated forty years of change in the bulrush marshes of the St. Lawrence Estuary and assessed the impact of the greater snow goose using IKONOS satellite imagery and aerial photographs. Baschuk et al. (2012) used satellite imagery to assess macrophyte response to water-level manipulations in the Saskatchewan River Delta of Manitoba. Delgado and Marin (2013) estimated swan habitat area changes at the Carlos Anwandter Sanctuary in Southern Chile by means of Normalized Difference Vegetation Index based on Landsat images.

However, it is not an easy task to accurately define wetland shoreline and capture or detect its change precisely because of the inherent spatial and temporal dynamic nature of this boundary. The characterization of shoreline change has inherent errors that depend upon several factors including offsets between different shoreline indicators or proxies, accuracy in shoreline measurement, shoreline temporal variability, number of data points (measured shoreline positions), non-uniform interval of time between shoreline measurements, total time span of shoreline data acquisition as well as the uncertainty of adopted comparing method itself (Maiti and Bhattacharya 2009; Yan et al. 2009). For these reasons, although extensive and outstanding works have been done to characterize wetland shoreline changes, many researches mainly focused on traditional qualitative or semi-qualitative analysis of man-delineated shoreline change between designated time interval rather than quantitative detection with error assessments based on multi-temporal shorelines extracted from digital images. Recent advancements in remote sensing have become increasingly important since land and sea interface could be well determined through the processing of multi-spectral band images (Ekercin 2007; Durduran 2010; Kuleli et al. 2011). Remote sensing techniques can be effective for extracting and acquiring reliable and consistent information with cost effectiveness, reduction in manual error and absence of subjectivity prior to conventional field techniques (Durduran 2010). Furthermore, statistical methods like linear regression has been found to be more reliable for multi-temporal shoreline change than many previous methods like end point rate (EPR) (Fenster et al. 1993), average of rates (AOR), and jackknife (JK) (Dolan et al. 1991) as minimizing potential random error and cyclical changes through a statistical approach (Maiti and Bhattacharya 2009; Kumar, et al. 2010; Kuleli et al. 2011).

In this work, four coastal wetlands of interest along Bohai rim including Liaohe Estuary, namely Shuangtai Estuary wetland, located in the coastal zone of Liaodong Bay, Haihe Delta wetland, built by the hydrologic discharge of Haihe River system located in Tianjin district of Bohai Bay, Yellow River Delta wetland, formed by sediments deposited by the Yellow River and its frequently course shifting process located between Bohai Bay and Laizhou Bay, and the foreshore wetland area of East Laizhou Bay were investigated in terms of shoreline changes. Natural processes including sedimentation, deposition, erosion and anthropogenic activities such as coastal agriculture, coastal engineering, land claim, dredging have caused apparent morphological changes (advance or retreat) to shoreline along these coastal wetlands. Therefore, the main purpose of this work was to detect shoreline changes in these wetlands using remote sensing and statistical techniques, and attempted to explore contributed factors that might affecting the resulted observations.

## Study Sites

Bohai (Fig. 1) is a shallow inner sea located between 37°07′ N~41°0′N, 117°35′~121°10′E in the east continent of China, with water surface area about 77284 km$^2$, average water depth 18 m and maximum depth 78 m. It is surrounded by Liaodong peninsula and Shandong peninsula connecting to open waters through Bohai straight. (Fig. 1).Coast zone of Bohai stretching from Laotieshan of Liaodong peninsula to Penglai of Shandong peninsula is mainly composed of three bays namely Liaodong bay, Bohai bay and Laizhoubay, respectively. With hydrologic discharges of several large rivers including Liaohe, Haihe and Yellow River, large area of coastal wetlands have been developed along Bohai rim especially in delta and estuarine areas. These wetlands not only provide indispensable habitats for various kinds of coastal plants for instance *Phragmites*, *Suaeda*, *Ailanthus altissima*, *Ulmus pumila* and wild animal lives such as *birds*, *mannalia*, *reptiles*, *amphibian*, *fishes*, *insects*, but also play

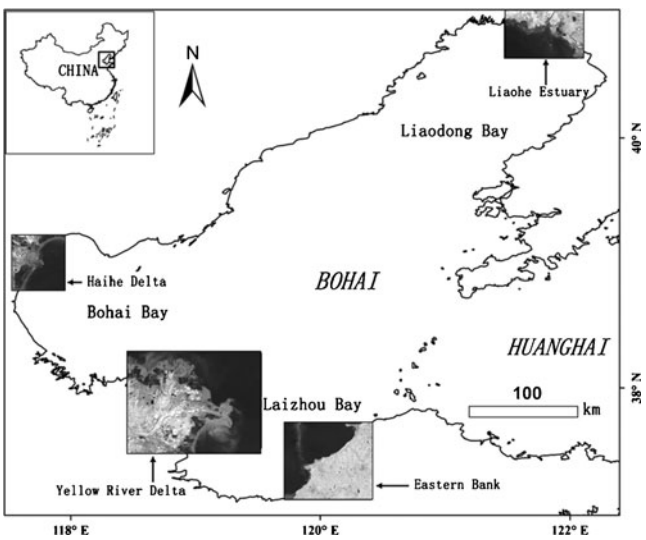


**Fig. 1** Location of the study sites

an important role in water purification, flood buffering as substitute of dams, losses reduction from storms and other extreme climate events.

Liaohe Estuary or Shuangtai Estuary wetland situated in the north of Liaodong Bay (Fig. 1), is one of 41 wetlands listed in the Record of Important International Wetland Conservation Districts (Ramsar site no.1441) in China, has 1280 $km^2$ natural and artificial wetlands with an elevation between 0 m and 10 m. It has abundant ecological resources including both unique vegetations and rare wild animal communities. There are 411 vertebrate species in the wetland, among which bird amount to 259, it is also the southern boundary for the wild red crowned crane to reproduce and propagate (Wang et al. 2008). Anthropogenic activities occurring here include fishery cultivation, recreation tourism and conservation education. Remains of nearby cities and industrial districts are found in some places within this region. Non-point coastal agricultural pollution and proposed engineering constructions also constitute potential treats to natural wetlands.

Haihe Delta located in the west of Bohai Bay covering an eastern area of Tianjin coast (Fig. 1), has an elevation between 0 m and 30 m above sea level. National natural reserve established and approved by the central government of China in 1992 occupying an area of 990 $km^2$ within this region. So far 196 vegetation species belonging to 121 generas and 46 families have been found so far in the reserve, most of which are herbaceous plants with few woody plants and shrubs (Xie et al. 2010). Artificial wetlands like cultivating wetlands are gradually taking place with natural types, continuously diminishing the habitat of wild communities. Recently, due to rapid expansion of Binhai New District of Tianjin, which is one of the fastest economic developing regions in North China emerging as the prominent commercial, industrial and shipping centre, vast natural wetlands are converting to artificial or solid dry lands by land reclamations. The consequence of habitat shrinking or damaging can lead to inevitable decrease of ecosystem biodiversity in this region.

Yellow River Delta located between Bohai Bay and Laizhou Bay with an area of 6010 $km^2$ (Fig. 1), is one of the most active regions of land-ocean interaction among the large river deltas in the world. The large areas of shallow sea and bog, an abundance of wetland vegetation and aquatic biological resources provide the birds with an exceptional habitat for breeding, migrating, and wintering, making this region an important stopover in the inland of Northeast Asia and around the western Pacific Ocean for bird migration. The total area of the wetlands amounts to 4167 $km^2$, or 69.3 % of the Yellow River Delta, including both natural wetland (bottomland of the Yellow River, newly formed wetland of the river mouth, coastal wetland, water-gathering swamp of the depressions, water bodies such as rivers and pools) and artificial wetland (such as paddy fields and salt pants) (Xiao and Li 1999). In recent years, the rate of sedimentation has slowed down and coastal erosion has increased, because the discharge of Yellow River often decreases as well as its sediment load during low water seasons (Xu et al. 2004; Cui and Li 2011). Besides, human activities like coastal constructions or seawall reinforcement also have influences on morphological variations of wetland shoreline along some segments of this district.

Laizhou Bay wetland located in the East Laizhou Bay, established by Laizhou City in 2005, is a candidate wetland to be included in national wetland management under protection in China. It is mainly composed of mudflats, dunes, beaches, seasonal marshes and wood areas with less developing delta. It is also an important stopover in the inland of Northeast Asia and around the western Pacific Ocean for birds and habitat for breeding, migrating, and wintering. This region is characterized by substantial mineral resources, popular tourist, dense population and intensive agricultural and industrial infrastructure. Tidal wetlands including marshes, sand dunes and beaches are suffering from coastal erosion problem due to accelerating of relative sea level rise and severe anthropogenic activities such as mineral exploration, water extraction, fish farming and other types of resource harvesting. These disturbances can alter natural conditions of coastal wetlands and the creatures' living space, diminishing the number of species, and populations of communities as well as biological diversity.

## Data and Methodology

### Landsat Data

To detect shoreline changes in above coastal wetlands along Bohai rim, a total of 28 Landsat series images acquired in different dates were used in our work. Landsat Muti-spectral Scanner (MSS), Thematic Mapper (TM) and Enhanced Thematic Mapper (ETM+) data have been widely used in wetland studies for many years because of their long record of global land-sea conditions with tens of meters spatial resolution. All images were rectified and projected using the Universal Transverse Mercator system in the world reference system (WGS84) datum with geographical error within 0.5 pixels. Further information about the specifications of satellite data in this work is listed in Table 1.

### Image Pre-processing and Shoreline Extraction

The methodology we used is to quantitatively detect multi-temporal shorelines extracted from Landsat series images (Fig. 2). According to the literature, data records of different

**Table 1** Specifications of Landsat images, tide data and errors estimated in the study

| Area | Satellite images | | | | | Tide conditions | | | | | | Error assessments | | | |
|---|---|---|---|---|---|---|---|---|---|---|---|---|---|---|---|
| | Date (mm/dd/yyyy) | Type | Path/row | Time (hh:mm:ss) | Pixel (m) | Time (hh:mm) | High tide height (m) | Tidal range (m) | Ebb tide duration (minutes) | Instantaneous tidal height (m) | Station | Measurement Error (m) | Proxy Offset (m) | Position Error (m) | Annualized Error (m) (m/year) |
| Liaohe Estuary | 09/05/1980 | MSS | 129/32 | 09:54:50 | 60 | 07:27 | 3.96 | 3.32 | 426 | 3.08 | Yingkou | 30 | 128.26 | 131.72 | 136.98 |
| | 09/18/1986 | TM | 120/32 | 09:55:13 | 30 | 05:55 | 4.05 | 3.44 | 424 | 1.98 | | 15 | 367.39 | 367.70 | |
| | 10/09/1988 | TM | 120/32 | 10:05:21 | 30 | 10:21 | 3.58 | 2.69 | 455 | 0.90 | | 15 | 602.17 | 602.36 | |
| | 09/11/1995 | TM | 120/32 | 09:36:54 | 30 | 12:41 | 3.62 | 2.54 | 425 | 2.10 | | 15 | 341.30 | 341.63 | |
| | 06/12/2000 | ETM+ | 120/32 | 10:26:37 | 28.5 | 11:12 | 3.20 | 2.52 | 381 | 3.14 | | 14.25 | 115.22 | 116.10 | |
| | 10/11/2006 | TM | 120/32 | 10:28:51 | 30 | 13:04 | 3.43 | 2.50 | 443 | 1.58 | | 15 | 454.35 | 454.60 | |
| | 07/15/2009 | TM | 120/32 | 10:23:35 | 30 | 14:16 | 3.88 | 2.93 | 453 | 2.48 | | 15 | 258.70 | 259.14 | |
| Haihe Delta | 05/29/1979 | MSS | 132/33 | 10:07:15 | 60 | 8:08 | 3.39 | 2.28 | 417 | 2.96 | Tanggu | 30 | 153.49 | 156.40 | 121.80 |
| | 06/15/1987 | TM | 122/33 | 10:12:04 | 30 | 12:45 | 3.45 | 2.19 | 378 | 2.04 | | 15 | 367.44 | 367.75 | |
| | 06/15/1993 | TM | 122/33 | 10:09:46 | 30 | 12:45 | 3.45 | 2.19 | 378 | 2.06 | | 15 | 362.79 | 363.10 | |
| | 10/11/1995 | TM | 122/33 | 09:48:07 | 30 | 11:42 | 3.38 | 1.95 | 403 | 1.81 | | 15 | 420.93 | 421.20 | |
| | 09/01/2001 | ETM+ | 122/33 | 10:36:11 | 28.5 | 15:59 | 3.93 | 3.10 | 341 | 3.90 | | 14.25 | −65.12 | 66.66 | |
| | 09/04/2005 | TM | 122/33 | 10:35:38 | 30 | 5:08 | 3.90 | 2.64 | 410 | 1.52 | | 15 | 488.37 | 488.60 | |
| | 08/30/2009 | TM | 122/33 | 10:37:03 | 30 | 14:52 | 3.83 | 3.01 | 380 | 3.10 | | 15 | 120.93 | 121.86 | |
| Yellow River Delta | 05/27/1979 | MSS | 130/34 | 10:02:07 | 60 | 15:38 | 1.15 | 0.79 | 338 | 1.14 | Dongying Harbor | 30 | 800.00 | 800.56 | 360.98 |
| | 08/11/1987 | TM | 121/34 | 10:07:39 | 30 | 04:51 | 1.49 | 0.85 | 370 | 0.64 | | 15 | 1633.33 | 1633.40 | |
| | 08/24/1992 | TM | 121/34 | 10:04:09 | 30 | 16:23 | 2.01 | 1.47 | 362 | 1.86 | | 15 | −400.00 | 400.28 | |
| | 09/18/1995 | TM | 121/34 | 09:43:32 | 30 | 13:13 | 1.81 | 1.30 | 371 | 1.45 | | 15 | 283.33 | 283.73 | |
| | 05/02/2000 | ETM+ | 121/34 | 10:34:00 | 28.5 | 07:35 | 1.38 | 0.91 | 403 | 1.00 | | 14.25 | 1033.33 | 1033.43 | |
| | 10/02/2006 | TM | 121/34 | 10:35:43 | 30 | 12:59 | 1.87 | 1.43 | 364 | 0.93 | | 15 | 1150.00 | 1150.10 | |
| | 09/11/2010 | TM | 121/34 | 10:31:57 | 30 | 05:53 | 1.61 | 0.42 | 348 | 1.22 | | 15 | 666.67 | 666.84 | |
| | 05/26/1979 | MSS | 129/34 | 9:55:40 | 60 | 14.54 | 0.77 | 0.36 | 358 | 0.76 | Longkou Harbor | 30 | 37.68 | 48.16 | 16.33 |

**Table 1** (continued)

| Area | Satellite images | | | | | Tide conditions | | | | | Error assessments | | | |
|---|---|---|---|---|---|---|---|---|---|---|---|---|---|---|
| | Date (mm/dd/yyyy) | Type | Path/row | Time (hh:mm:ss) | Pixel (m) | Time (hh:mm) | High tide height (m) | Tidal range (m) | Ebb tide duration (minutes) | Instantaneous tidal height (m) | Station | Measurement Error (m) | Proxy Offset (m) | Position Error (m) | Annualized Error (m) (m/year) |
| East Laizhou Bay | 09/18/1986 | TM | 120/34 | 9:56:01 | 30 | 13:00 | 1.31 | 0.94 | 353 | 0.84 | | 15 | 26.09 | 30.27 | |
| | 08/31/1991 | TM | 120/34 | 9:57:50 | 30 | 11:35 | 1.05 | 0.58 | 328 | 0.59 | | 15 | 62.32 | 64.10 | |
| | 09/11/1995 | TM | 120/34 | 9:37:41 | 30 | 05:55 | 0.79 | 0.23 | 348 | 0.63 | | 15 | 56.52 | 58.48 | |
| | 06/12/2000 | ETM+ | 120/34 | 10:27:24 | 28.5 | 05:09 | 1.32 | 0.85 | 376 | 1.18 | | 14.25 | −23.19 | 27.22 | |
| | 10/27/2006 | TM | 120/34 | 10:29:49 | 30 | 10:03 | 1.04 | 0.63 | 346 | 1.03 | | 15 | −1.45 | 15.07 | |
| | 07/15/2009 | TM | 120/34 | 10:24:23 | 30 | 08:10 | 0.89 | 0.34 | 335 | 0.79 | | 15 | 33.33 | 36.55 | |

remote sensors are not directly comparable especially in quantitative remote sensing research because there are time differences in image acquisition, signal variations of exo-atmospheric solar irradiance arising from spectral band distinctions, and atmospheric effects of aerosol scattering under various weather conditions on image acquisition dates (Kuleli et al. 2011). Image pre-processing including radiometric calibration and atmospheric correction is necessary to get comparable data at the same level (Chander et al. 2009; Tyagi and Bhosle 2011). Therefore, digital numbers recorded by Landsat images were transformed to top of atmosphere reflectance according to Eq. 1 and then converted to ground surface reflectance using simple atmospheric correction of dark object subtraction according to Eq. 2:

$$Rrs_{TOA} = \pi L_\lambda d^2 / (E_\lambda \cos\theta_s) \quad (1)$$

$$Rrs_{GSR} = Rrs_{TOA} - \alpha \quad (2)$$

Where $Rrs_{TOA}$ refers to planetary top of atmosphere reflectance, $\pi$ is mathematical constant equal to ~3.14159; $L_\lambda$ is spectral radiance at sensor's aperture (W $m^{-2}$ $sr^{-1}$ $\mu m^{-1}$);

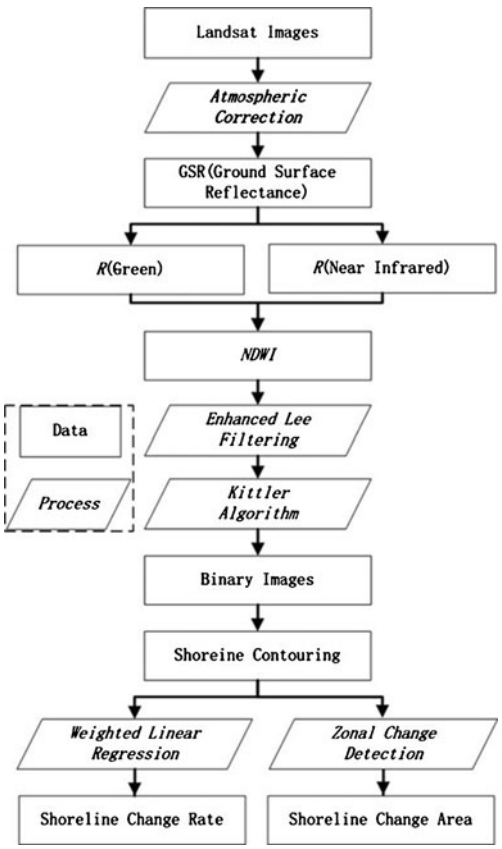


**Fig. 2** Flow chart of automatic shoreline extraction and shoreline change calculation

d is Earth-Sun distance (astronomical units). $E_\lambda$ refers to mean exo-atmospheric solar irradiance (W $m^{-2}$ $sr^{-1}$ $\mu m^{-1}$) and $\theta_s$ is solar zenith angle. $Rrs_{GSR}$ refers to ground surface reflectance, $\alpha$ is the minimum reflectance value of near infrared band within deep water area.

In order to extract wetland shorelines through land-water segmentation, we need to prepare index images of interested area with the maximum discrepancy in land and sea. *NDWI* index has proved to be effective in increase the contrast between land and water feature by maximizing water reflectance in green and soil or vegetation feature in *NIR* (Sezgin and Sankur 2004). *NDWI* gray images were generated according to Eq. 3:

$$NDWI = (Green - NIR)/(Green + NIR) \quad (3)$$

Where *Green* is the green band such as MSS band 1 or TM/ETM + band 2, and *NIR* is the near infrared band such as MSS band 3 or TM/ETM + band 4. The generated *NDWI* images were further enhanced through the enhanced Lee filtering in order to suppress possible speckle noises while preserving the edge information of image features (Lee 1981).

Next was to perform automatic wetland shoreline extraction from enhanced *NDWI* images. So far many techniques have been developed to extract shorelines from remote sensing images. Manual, image enhancement, comparison of two independent land cover classifications, density slice using single or multiple bands multi-temporal or multi-spectral classification, both supervised and unsupervised (e.g. IDOSATA, PCA, Tasseled Cap) are most common techniques (Ryu et al. 2002). Besides, several image processing algorithms such as pre-segmentation, segmentation and post-segmentation have also been used (Liu and Jezek 2004; Kuleli et al. 2011; Josep et al. 2012). In this work, an automatic binarization method Kittler threshold algorithm was utilized on filtered *NDWI* gray images to delineate shoreline of coastal wetlands. The principle of this algorithm is to derive appropriate thresholds by the minimum error criterion through dynamic clustering (Kittler and Illingworth 1986). It is a robust and rapid algorithm dealing with images that have bimodal distribution histogram like *NDWI* images generated here. As a result, *NDWI* images were separated into constituent homogeneous regions. The bordering pixels between segmented land and water regions of the produced binary images could be differentiated from other objects and traced into shoreline vector files for shoreline change analyzing.

## Detecting Changes of Multi-temporal Shorelines

We carried out alongshore shoreline change rate and shoreline change area detection for identified sections that behaved significant area variations. It is important to determine an appropriate method for detecting shoreline change rates of multiple coastal wetland shorelines. Because as mentioned in section 1, the characterization of shoreline changes have inherent uncertainties that depend upon offsets between different shoreline indicators or proxies, measurement errors from data sources that determine the accuracy of each shoreline position, sampling errors that account for the local variability of true shoreline positions in short term, and statistical errors associated with compiling and comparing shoreline positions (Maiti and Bhattacharya 2009; Yan et al. 2009). Linear regression has been found to be reliable for analysis of multiple shorelines. Rates of shoreline change were slopes of the least-squares regression lines fitted to the intersection points of multiple shorelines and their corresponding transects casted perpendicular to them (Thieler et al. 2005; Genz et al. 2007; Maiti and Bhattacharya 2009; Kumar, et al. 2010; Kuleli et al. 2011). We utilized weighted linear regression (WLR) to determine alongshore multi-temporal shoreline change rates. WLR assumes heteroscedastic uncertainties and it means that the variance associated with each Y component (wetland shoreline position) is usually not the same at each X component (different data acquisition time), if the variance ($E_{sp}^2$) or standard deviation ($E_{sp}$) for each shoreline position is known, the weight ($w$) is equal to $1/E_{sp}^2$ (Thieler et al. 2005; Genz et al. 2007). Greater emphasis is placed on data points which the position uncertainty is smaller. Here $E_{sp}$ denotes the standard deviation for each shoreline position standing for total shoreline position uncertainty by taking the square of the sum of the squares of measurement error ($E_m$) and shoreline proxy offset ($E_p$). So total shoreline position uncertainty is written in the form of Eq. 4:

$$E_{sp} = \sqrt{E_m^2 + E_p^2} \quad (4)$$

$E_m$ represents the maximum acceptable rectification error of Landsat images (Table 1). $E_p$ is the calculated maximum horizontal offset between instantaneous waterlines (*IWL*, image shorelines) and the mean high waterlines (*MHWL*, true shorelines) in these wetlands (clarified later). In this way a separate $E_{sp}$ can be calculated for each period, and these values can be annualized to provide an best error estimation $E_a$ for the shoreline change rates at a specific wetland (Table 1). The annualized error ($E_a$) is calculated by Eq. 5:

$$E_a = \frac{\sqrt{\sum E_{spi}^2}}{time} \quad (5)$$

According to previous studies, tidal heights corresponding to instantaneous waterlines extracted from images can be calculated if the tidal station records of satellite over-

passing dates are available, then local wetland slope can be deduced from the maximum and minimum instantaneous tidal heights we have calculated, at last the horizontal distances between *MHWL* and maximum *IWL* namely shoreline offsets can be obtained based on both their tidal heights and the deduced slope values (Mason et al. 1995; Mason et al. 1997; Ryu et al. 2002; Shen et al. 2008; Yan et al. 2009). We achieved the horizontal distances namely shoreline offsets $E_p$ between different waterlines (*IWL* and *MHWL*) using this 'waterline' method:

$$E_p = (H - h_{\max})/\tan\theta \quad (6)$$

$H$ is the mean high tide record of nearby tidal station; $h_{max}$ and $\theta$ are the calculated local maximum value of instantaneous tidal heights and shoal slope according to Eqs. 7 and 8:

$$h = H' - R/2 \times [1 - \cos(t/T \times 180)] \quad (7)$$

$$\theta = \arctan[(h_{\max} - h_{\min})/d] \quad (8)$$

In Eq. 7, $H'$ and $R$ refer to station records of high tide height and tidal range on each image acquisition date; $t$ is the time lag between high tide and image taking time on each date and $T$ refers to recorded ebb tidal duration. In Eq. 8, $h_{max}$ and $h_{min}$ are the calculated maximum and minimum value of tidal height of instantaneous waterlines, the distance between them is measured and denoted as $d$. The tide data listed in Table 1 for $E_p$ estimation were provided by China Oceanic Information Network affiliated to the State Oceanic Administration People's Republic of China.

In this study, proxy offsets accounting for tidal effects are the offsets between extracted image shorelines (instantaneous waterline, *IWL*) and local true shoreline (mean high waterline, *MHWL*), measurement errors are the maximum rectification errors of satellite images of each sensor type, sampling errors are not incorporated into uncertainty due to the limitation in collection of high frequency local data regarding short–term variability of true shoreline position at most coastal fields, statistical errors are the variability around the regression trend line, representing a 90 % confidence interval for the slope of the regression line implying that with 90 % statistical confidence the true rate of shoreline change falls within the range defined by the computed values plus or minus the error value. Statistical errors reflect both proxy offsets and measurement errors. Estimates of the maximum errors are provided in Tables 1 and 2 to show how each error contributes to uncertainty in the shoreline position and in the result of change rates. Results of shoreline change rates (retreat or advance) computed along four coastal wetlands are shown in Figs. 3 to 6. For coastal sections that behaved significant area variations rather than merely alongshore perpendicular changes, their areas were determined by zonal change detection and the results were illustrated in Fig. 7.

## Results

Table 2 shows statistical results of shoreline change rates on different segment of coastal wetlands along Bohai rim. All wetland areas were divided into three segments according to their specific coastal morphology. We found that although there were statistical uncertainties leading by data rectification and proxy offset of ocean tide action, dominant trends of the shoreline changes could be detected and sections that have significant area changes were identified from satellite images.

### Shoreline Changes in Liaohe Estuary Wetland

For wetland of Liaohe Estuary, it had an average retreat trend and advance trend of −40.3 m/year (92 %) and 10.0 m/year (8 %) in long term. While in short term, it showed an average retreat trend of −119.2 m/year (98 %) and an advance trend of 35.0 m/year (2 %) over 74 transects (Fig. 3). Shoreline changes were found to be much more significant in river flanks (A and C) than river mouth (B), with the maximum withdraw distance of 3,423 m in section C. Zonal change detection on section A and section C showed that the retreated shoreline areas amount to 35.1 $km^2$ and 90.7 $km^2$, at an average speed of 1.2 $km^2$/year and 3.0 $km^2$/year (Fig. 7a, b). The extent of shoreline changes for Liaohe Estuary wetland was much more significant in the latest four periods than long term, with a dominated landward retreating trend along this region (Fig. 3). The accelerated retreating process revealed here might be related with severe land dredging activities on riverbed and foreshore due to fishery cultivation and nearby industrial constructions in recent years. These land dredging activities could not only deform river channel but also directly decrease runoff and the volume of sediments that should be transported to depositing in the coastal area.

### Shoreline Changes in Haihe Delta Wetland

Shoreline of Haihe Delta wetland showed an average retreat trend of −9.9 m/year (15 %) and advance trend of 58.6 m/year (85 %) in long term and it had an average retreat trend of −115.1 m/year (21 %) and an average advance trend of 224.6 m/year (79 %) in short term (Fig. 4). For this area, shoreline in the middle segment (B) had a dramatic seaward expansion than both sides (A and C), with a maximum advance distance of 14,836 m in section B, which behaved no retreat. Result of zonal change detection

**Table 2** Summary of shoreline variation statistics for four coastal wetlands

| Area | A | B | C | Mean |
|---|---|---|---|---|
| Liaohe Estuary | | | | |
| Retreat trend[a] (m/year) | −38.3±25.9 | −11.1±10.4 | −71.4±61.5 | −40.3±32.6 |
| % | 34 | 14 | 44 | |
| Retreat trend[b] (m/year) | −84.0±73.6 | −23.0±21.9 | −250.7±231.5 | −119.2±109.0 |
| % | 34 | 18 | 46 | |
| Advance trend[a] (m/year) | – | 2.3±2.1 | 17.6±16.1 | 10.0±9.1 |
| % | – | 5 | 3 | |
| Advance trend[b] (m/year) | – | 14.3±12.7 | 55.7±52.1 | 35.0±32.4 |
| % | – | 1 | 1 | |
| Number of transects (74) | 25 | 14 | 35 | |
| Haihe Delta | – | | | |
| Retreat trend[a] (m/year) | −11.7±16.7 | | 8.0±8.0 | −9.9±12.4 |
| % | 9 | – | 6 | |
| Retreat trend[b] (m/year) | −124.5±121.6 | - | −105.6±104.3 | −115.1±113.0 |
| % | 12 | – | 9 | |
| Advance trend[a] (m/year) | 14.3±30.5 | 146.5±133.4 | 15.1±10.6 | 58.6 ±58.2 |
| % | 9 | 72 | 4 | |
| Advance trend[b] (m/year) | 103.9±101.3 | 512.3±506.8 | 57.5±50.6 | 224.6±219.6 |
| % | 6 | 72 | 1 | |
| Number of transects (78) | 14 | 56 | 8 | |
| Yellow River Delta | | | | |
| Retreat trend[a] (m/year) | −115.3±106.9 | −44.0±49.1 | −121.7±172.2 | −93.7±109.4 |
| % | 28 | 21 | 32 | |
| Retreat trend[b] (m/year) | −114.0±109.5 | −26.7±28.1 | −82.7±86.9 | −74.5±74.8 |
| % | 28 | 18 | 21 | |
| Advance trend[a] (m/year) | 35.0±68.3 | – | 117.1±131.9 | 76.1±100.1 |
| % | 3 | – | 16 | |
| Advance trend[b] (m/year) | 22.7±40.3 | 10.9±15.7 | 152.4±170.6 | 62.0±75.6 |
| % | 3 | 3 | 27 | |
| Number of transects (194) | 60 | 40 | 94 | |
| East Laizhou Bay | | | | |
| Retreat trend[a] (m/year) | −2.6±1.8 | −2.7±2.5 | – | −2.7±2.2 |
| % | 4 | 32 | – | |
| Retreat trend[b] (m/year) | −1.6±0.7 | −3.4±2.3 | – | −2.5±1.5 |
| % | 5 | 31 | – | |
| Advance trend[a] (m/year) | 12.3±10.5 | 1.9±2.2 | 44.1±22.5 | 19.4±35.2 |
| % | 44 | 1 | 19 | |
| Advance trend[b] (m/year) | 8.9±6.1 | 0.7±1.2 | 36.4±16.8 | 15.3±8.0 |
| % | 43 | 2 | 19 | |
| Number of transects (124) | 60 | 40 | 24 | |

Trend[a] is long term result calculated from all periods; Trend[b] is short term result calculated from the latest four periods; % denotes the percentage of changed transects in all transects of each wetland

showed that the area expansion of section B amounts to 146.1 km$^2$ in the past 3 decades, with an average expansion rate of 4.9 km$^2$ per year (Fig. 7c). For shoreline variation of this region, it was mainly dominated by a seaward advancing trend and the rate of change was far more dramatic in recent periods especially in the middle segment, which is the most rapid expansion area of Binhai New District in Tianjin City due to fast economic development (Fig. 4). Vast area of coastal natural wetlands especially tidal wetlands were lost and converting to artificial or solid dry lands caused by land reclamation during the process of quick development. The consequence of habitat shrinking or damaging can lead to inevitable decrease of ecosystem biodiversity in this area.

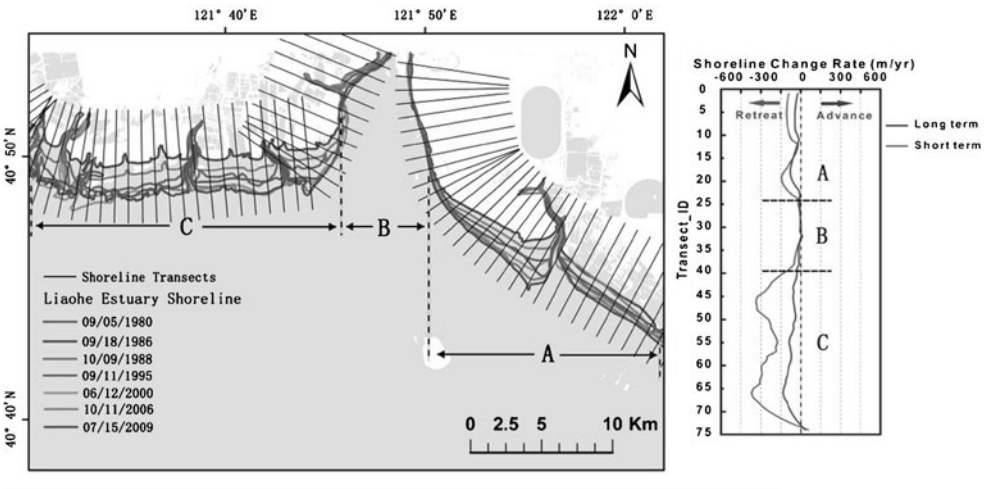


**Fig. 3** Shoreline changes in wetland of Liaohe Estuary

## Shoreline Changes in Yellow River Delta Wetland

Results of shoreline changes in the wetland of Yellow River Delta showed that the average long term retreat and advance trend were −93.7 m/year (81 %) and 76.1 m/year (19 %) while in short term the average retreat trend was −74.5 m/year (67 %) and the mean advance trend was 62.0 m/year (33 %) (Fig. 5). Section A of this region behaved much more significant landward retreat than section B, which had no obvious change. The maximum extent of seaward advance occurred in section C was 16,716 m. Results of zonal change detection showed that, the landward retreat area of section A was 161.69 km$^2$, at an average speed of 5.1 km$^2$ per year (Fig. 7d). The seaward advance area of section C was 502.3 km$^2$, with an average rate of 15.7 km$^2$ per year (Fig. 7e). With similar evolution trends both in short and long term, the wetland of Yellow River Delta was observed to be suffering from coastal erosion problem in some segment of this area except those areas that had been stabilized by seawall (section B) and the current mouth of river (section C). The coastal erosion phenomenon occurring here is believed to be related with the decreased discharge of Yellow River and the sediment load it carried during low water seasons. It would diminish the space area of living, breeding, migrating, and wintering for wild wetland species.

## Shoreline Changes in East Laizhou Bay Wetland

The mean retreat and advance trend in wetland of East Laizhou Bay was −2.7 m/year (36 %) and 19.4 m/year (64 %) in long term. The retreat and advance trend on average was −2.5 m/year (36 %) and 15.3 m/year (64 %) in short term. Shoreline variations of section A and C were shown to be more significant than section B (Fig. 6). The maximum advance distance occurred in C was 2,839 m. Zonal change detection showed that in the past three decades the expanded area was 9.81 km$^2$ with a rate of 0.3 km$^2$ every year (Fig. 7f). Variations of shoreline along East Laizhou Bay revealed that besides minor erosion occurring in the middle part, seaward advance was the dominated process for both long and short periods (Fig. 6). The losses of sand dunes and beaches in the middle segment is likely to be attributed with accelerated relative sea level rise and land

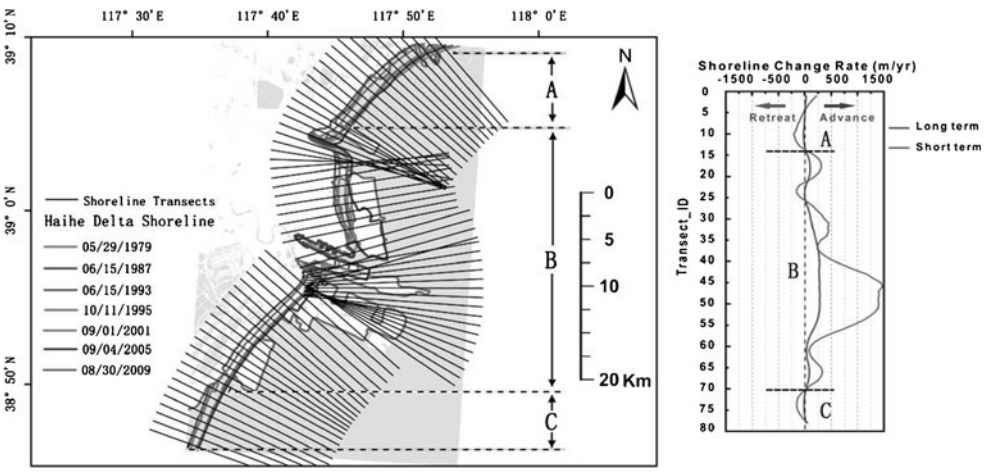


**Fig. 4** Shoreline changes in wetland of Haihe Delta

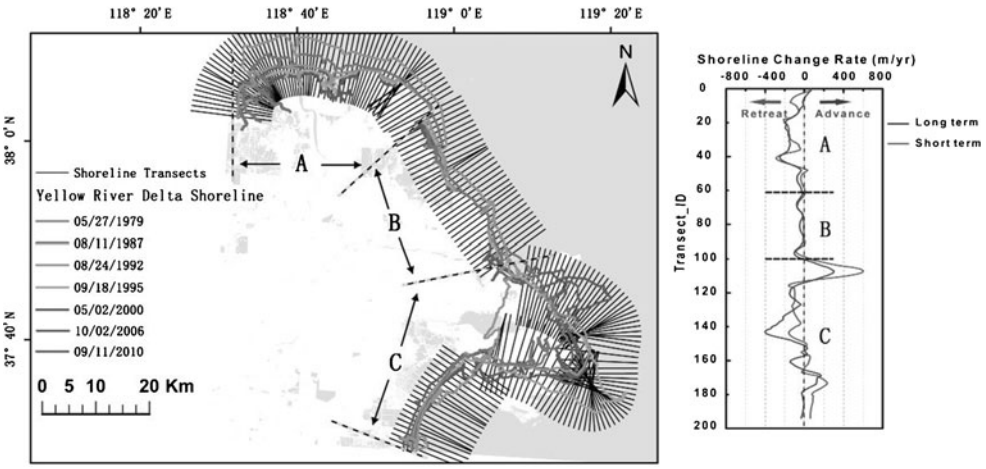


**Fig. 5** Shoreline changes in wetland of Yellow River Delta

subsidence because of underground water extraction and mineral exploration, while seaward advance is mainly due to severe anthropogenic activities such as industrial expansion and harbour construction. These disturbances can alter natural conditions of coastal wetlands and the creatures' living space, diminishing the number of species, and populations of communities and biological diversity.

## Discussions

Coastal wetlands of Bohai rim represent some of the most functional and ecological habitats, and they also constitute valuable natural resources in China. These ephemeral interfaces between water and land are sometimes also the sites of intense residential and commercial development even though they are frequently subjected to natural hazards including flooding, storm impacts, and coastal erosion. Because population centers continue to shift toward the coast making valuable coastal wetlands more vulnerable, a detection of coastal wetland shoreline changes was conducted in this research. As coastal wetland shoreline change is one of the most important indications of land-ocean interaction processes in complex and dynamic coastal zones, therefore using shoreline position as a proxy for wetland change is easily understood by those who are interested in historical movement of wetlands.

In this study, shorelines of four coastal wetlands of Bohai rim were extracted from remote sensing images using automatic segmentation algorithm. Long term and short term shoreline change rates were determined using weight linear regression method. Areas of wetlands that had significant changes were identified using zonal change detection. Results showed that shoreline changes including retreat and advance have caused significant morphological changes to the coastal wetlands of Bohai rim. Overall, the shoreline of Liaohe Estuary wetland was dominated by a landward retreating trend along most segments of this region (Fig. 3). This retreating process might be a result of both natural and anthropogenic factors. It might be related with severe land dredging activities on riverbed and foreshore due to fishery cultivation and nearby industrial constructions in recent years (Zhan et al. 2010). These land dredging activities could not only deform river channel but also directly decrease runoff and the volume of sediments that should be transported to depositing in the coastal area. It

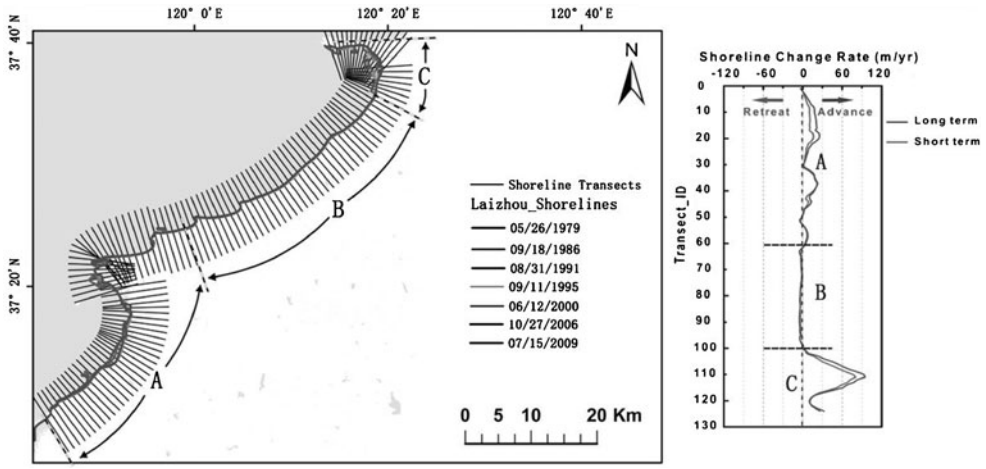


**Fig. 6** Shoreline changes in wetland of East Laizhou Bay

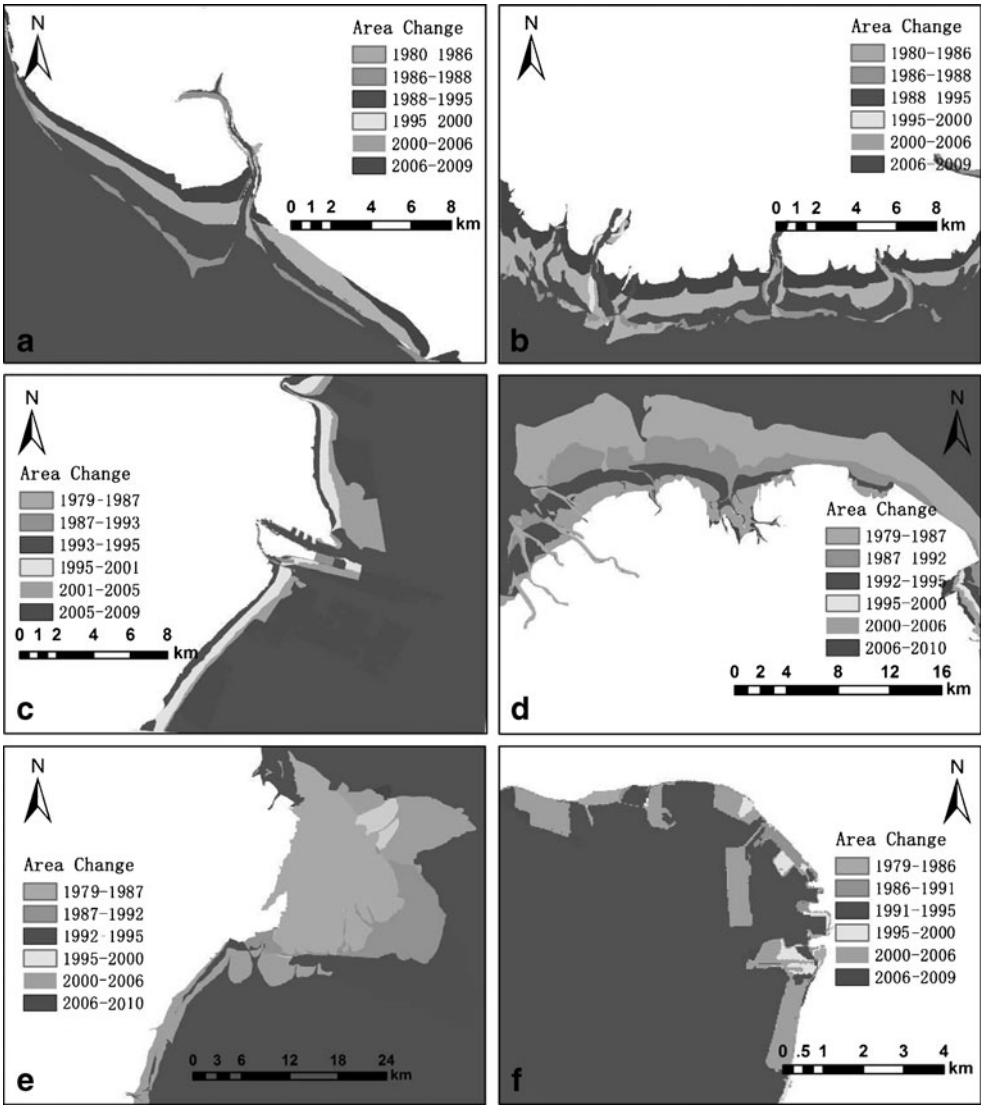


**Fig. 7** Results of zonal change detection: (**a**) Section A in Liaohe Estuary (**b**) Section C in Liaohe Estuary (**c**) Section B in Haihe Delta (**d**) Section A in Yellow River Delta (**e**) Section C in Yellow River Delta (**f**) Section C in East Laizhou Bay

was reported that the yearly average runoff and sediment load of Liaohe downstream have been decreased to about 10 % of previous level since 2000 (Guo and Guo 2010). Relative sea level rise might also contribute to the retreating process occurred in this region, Xiao et al. (2003) showed that the rate of relative sea level rise was estimated to be 5~6 mm/a according to the observation data of Yingkou tide station from 1965 to 1995 and the trend of sea level rise seems to be accelerating in recent decades (Zhan et al. 2009). For shoreline of Haihe Delta wetland, it was mainly dominated by a rapid seaward advancing trend especially in the middle segment (Fig. 4). Shoreline changes within this region were mainly driven by population growth and quick urban expansion during economic development (Xie et al. 2010; Liu et al. 2012). The loss of coastal natural wetlands especially tidal wetlands land reclamation activities would cause inevitable decrease of ecosystem biodiversity in this area. It is wise to take biodiversity conservation into consideration in future city planning. The wetland of Yellow River Delta was observed to be suffering from coastal erosion problem except section B that had been stabilized by seawall and current mouth area within section C (Fig. 5). Cui and Li (2011) reported that the variation in runoff and sediment have great impacts on erosion-accretion pattern in Yellow River estuary. The erosion in section A is due to lack of steady sediment supply because course of Yellow River has shifted since 1976. For section B, the built seawall prevents shoreline from waves, tides and current actions and relieves sediment losses within this area. The shoreline variations in section C is believed to be closely related with the variation of runoff and sediment load caused by constantly course shifting process during the past thirty years (Cui and Li 2011; Li et al. 2012). It should be noted that coastal erosion occurred in this region would diminish the space area of wild wetland species and effective ecological engineering might be helpful to relieve the stress of this problem. Variations of shoreline along East Laizhou Bay showed except the erosion segments of the middle part,

seaward advance was the dominated process in this region (Fig. 6). The coastal erosion phenomenon occurring here is attributed to the construction of man-made structures along upstream rivers which could trap sediment and diminish the amount of sand supplied by watersheds to the littoral system (Du and Sun 2005). Besides, coastal sand dredging activities directly cause sand dunes diminishing. Furthermore, local rise in relative sea level caused by subsidence because of underground resource exploration or extraction (mine, gold, gas, oil, water) might also contribute to coastal erosion of this district (Du et al. 2007). Seaward advance is mainly due to severe anthropogenic activities such as industrial expansion and harbour construction. Both natural and human disturbances occurring here could alter the living conditions of coastal wetlands and would decrease the habitat suitability for wetland ecological communities.

## Conclusions

According to the findings of this research, to relieve the environmental stresses caused by natural processes and human activities, ecological management plans of coastal wetlands should be considered to incorporate with regional or national management projects by decision makes in the future. Wetland area of Liaohe Estuary, Haihe Delta, Yellow River Delta and East Laizhou Bay should be preserved to avoid unrecoverable changes leading by negative human impacts on their unique coastal environment. Public awareness of these ecologically important regions should be raised by authority to keep these wetlands from agricultural and industrial practices. New regulations and further studies are also needed to protect and regularly monitor the spatial and temporal changes of coastal wetlands in our country.

Coastal wetland shoreline movement is a complex phenomenon that is the result of both natural processes and man-made effects. Successfully managing the coastal wetlands requires careful consideration of all the components of shoreline motion. Objectively, results of wetland shoreline change detection using extracted images shorelines are only as reliable as: (1) measurement errors that determine the accuracy of extracted each shoreline position, (2) offsets between different shoreline indicators, (3) sampling errors that account for the variability of shoreline position, (4) statistical errors associated with compiling and comparing shoreline positions. In this study, although there were statistical uncertainties leading by data rectification and proxy offset caused by ocean tide effect, dominant trends of coastal wetlands in Bohai rim during the past three decades were determined and revealed on the basis of multi-temporal historical shorelines extracted from Landsat images. While due to the insufficient availability of tidal data and access difficulty to specific site, detailed and accurately shoreline correction might be limited along designated coastal area, it is still practical to acquire important information about shoreline changes for coastal wetlands. Detailed field data accumulations are warranted in the long run.

The shoreline changes of coastal wetlands detected and interpreted in this work may help future studies to reveal the regional/national pattern and reasons for spatial-temporal changes in these areas. It is our anticipation that the result of this work would support wetlands protection and management in China's coast zone.

**Acknowledgments** This research is supported by the CAS Strategic Priority Research Program Grant No.XDA05130703 and the Knowledge Innovation of the Chinese Academy of Sciences No. KZCX2-YW-224. We would like to thank two anonymous reviewers and the associate editor for extremely helpful comments. We thank the China Oceanic Information Network and site data collection and processing staff for contributing to tidal station data, and the agencies and institutions that funded long-term records at these sites.

## References

Allard M, Fournier RA, Grenier M (2012) Forty years of changes in the Bulrush Marshes of the St. Lawrence Estuary and the impact of the greater snow goose. Wetlands 32:1175–1188

Baschuk MS, Ervin MD, Clark WR (2012) Using satellite imagery to assess macrophyte response to water-level manipulations in the Saskatchewan River Delta, Manitoba. Wetlands 32:1091–1102

Chander G, Markham BL, Helder DL (2009) Summary of current radiometric calibration coefficients for Landsat MSS, TM, ETM and EO-1 ALI sensors. Remote Sensing of Environment 113:893–903

Cui BL, Li XY (2011) Coastline change of the Yellow River estuary and its response to the sediment and runoff (1976–2005). Geomorphology 127:32–40

Delgado LE, Marin VH (2013) Interannual changes in the habitat area of the Black-Necked Dwan, Cygnus melancoryphus, in the Carlos Anwandter Sanctuary, Southern Chile: A remote sensing approach. Wetlands 33:91–99

Dolan R, Fenster MS, Holme SJ (1991) Temporal analysis of shoreline recession and accretion. Journal of Coastal Research 7:723–744

Du GY, Sun ZY (2005) Research of artificial geological disasters of coast belt in east bank of Laizhou Bay, Bohai Bay. Journal of Geological Hazards and Enviroment Preservation 16:225–230

Du GY, Wang Q, Wang QX et al (2007) Research advances on the marine-land interaction in coast of Laizhou Bay. Marine Sciences 31:66–71

Durduran SS (2010) Coastline change assessment on water reservoirs located in the Konya Basin Area, Turkey, using multitemporal landsat imagery. Environmental Monitoring and Assessment 164:453–461

Ekercin S (2007) Water quality retrievals from high resolution ikonos multispectral imagery: a case study in Istanbul, Turkey. Water, Air, and Soil Pollution 183:239–251

Fenster MS, Dolan R, Elder JF (1993) A new method for predicting shoreline positions from historical data. Journal of Coastal Research 9:147–171

Genz AS, Fletcher CH, Dunn RA, Frazer LN, Rooney JJ (2007) The predictive accuracy of shoreline change rate methods and

alongshore beach variation on Maui, Hawaii. Journal of Coastal Research 23:87–105

Ghanavati E, Firouzabadi PZ, Jangi AA, Khosravi S (2008) Monitoring geomorphologic changes using Landsat TM and ETM+data in the Hendijan River delta, southwest Iran. International Journal of Remote Sensing 29:945–959

Guo WD, Guo WZ (2010) Analysis of flow and sediment characteristics and influence factors in downstream of Liao River. Journal of Shenyang Agricultural University 41:360–362

Jiang Y, Li LF, Kang H, Zhong XB (2003) A remote sensing analysis of coastline change along the Bohai bay muddy coast in the past 130 years. Remote Sensing for Land & Resources 4:54–59

Josep EP, Jaime A, Luis AR (2012) Automatic extraction of shorelines from Landsat TM and ETM+multi-temporal images with sub pixel precision. Remote Sensing of Environment 123:1–11

Kittler J, Illingworth J (1986) Minimum error thresholding. Pattern Recognition 19:41–47

Kuleli T, Guneroglu A, Karsli F, Dihkan M (2011) Automatic detection of shoreline change on coastal Ramsar wetlands of Turkey. Ocean Engineering 38:1141–1149

Kumar A, Narayana AC, Jayappa KS (2010) Shoreline changes and morphology of spits along southern Karnataka, west coast of India: A remote sensing and statistics-based approach. Geomorphology 120:133–152

Lee JS (1981) Refined filtering of image noise using local statistics. Computer Graphics and Image Processing 15:380–389

Li XJ, Michiel CJ (2010) Coastline change detection with satellite remote sensing for environmental management of the Pearl River Estuary, China. Journal of Marine Systems 82:54–61

Li YZ, Yu JB, Han GX et al (2012) Coastline change detection of the Yellow River Delta by satellite remote sensing. Marine Sciences 36:99–106

Liu BX, Huang YH, Fu JY, Jiang D (2012) Analysis on spatial-temporal change and driving forces of land use in Tianjin harbour. Journal of Geo-Information Science 14:270–278

Liu C, JiangH HY, Zhang S, Su L, LiX PX, Wen Z (2010) Habitat changes for breeding waterbirds in Yancheng National Nature Reserve, China: A remote sensing study. Wetlands 30:879–888

Liu H, Jezek KC (2004) Automated extraction of coastline from satellite imagery by integrating Canny edge detection and locally adaptive thresholding methods. International Journal of Remote Sensing 25:937–958

Maiti S, Bhattacharya AK (2009) Shoreline change analysis and its application to prediction: A remote sensing and statistics based approach. Marine Geology 257:11–23

Mason DC, Davenport I, Flather RA (1995) Construction of an intertidal digital elevation model by the 'waterline' method. Geophysical Research Letters 22:3187–3190

Mason DC, Davenport I, Flather RA (1997) Interpolation of an intertidal digital elevation model from heighted shorelines: A case study in the western wash. Estuarine, Coastal and Shelf Science 45:599–612

Rahman AF, Dragoni D, El-Masri B (2011) Response of the Sundarbans coastline to sea level rise and decreased sediment flow: A remote sensing assessment. Remote Sensing of Enviroment 115:3121–3128

RAMSAR (2012) The Ramsar Convention on Wetlands. http://www.ramsar.org/. Accessed 8 July 2012

Rebelo LM, Finlayson CM, Nagabhatla N (2009) Remote sensing and GIS for wetland inventory, mapping and change analysis. Journal of Environment Management 90:2144–2153

Ryu J, Won J, Min KD (2002) Waterline extraction from Landsat TM data in a tidal flat. A case study in Gomso bay, Korea. Technical Report Series, vol. 83, Department of Geography and Anthropology Lousiana State University, pp 442–456

Shen F, Hao A, Wu JP (2008) A remotely sensed approach on waterline extraction of silty tidal flat for DEM construction, a case study in Jiuduansha shoal of Yantze River. Acta Geodaetica Et Cartographica Sinica 37:102–107

Sezgin M, Sankur B (2004) Survey over image thresholding techniques and quantitative performance evaluation. Journal of Electronic Imaging 13:146–165

Tyagi P, Bhosle U (2011) Atmospheric correction of remote sensed images in spatial and transform domain. International Journal of Image Processing 5:564–579

Thieler ER, Himmelstoss EA, Zichichi JL, Miller TL (2005) Digital Shoreline Analysis System (DSAS) version 3.0: an ArcGIS extension for calculating shoreline change. http://woodshole.er.usgs.gov/project-pages/DSAS/version3. Accessed 9 July 2012

Wang TL, Zhou LF, Yang PQ, Zhao B (2008) Study of Panjin Wetlands Along Bohai Coast: (I) the information system of wetlands based on 3S Technique. Journal of Ocean University of China 7:411–415

Xiao D, Li X (1999) Core concepts of landscape ecology. Journal of Environmental Science 11:131–135

Xiao DN, Han MK, Li XW, Liu YF (2003) Sea level rising around Bohai Sea and deltaic wetlands protection. Quaternary Sciences 23:237–246

Xie ZL, Xu XG, Yan L (2010) Analyzing qualitative and quantitative changes in coastal wetland associated to the effects of natural and anthropogenic factors in a part of Tianjin, China Estuarine. Coastal and Shelf Science 86(3):379–386

Xu XG, Lin HP, Fu ZY (2004) Probe into the method of regional ecological risk assessment-a case study of wetland in the Yellow River Delta in China. Journal of Environmental Management 70(3):253–262

Yan HB, Li BB, Chen MD (2009) Progress of researches in coastline extraction based on RS technique. Areal Research and Development 28:101–105

Zhan JG, Wang Y, Cheng YS (2009) The analysis of China sea level change. Chinese Journal of Geophysics 52:1725–1733

Zhan YZ, Fang GZ, Ni J, Hu K (2010) Reaserch on century's changes of coastlines of Liaohe Estuay. Journal of Marine Sciences 28:14–21